ELSEVIER

Organic Electronics 2 (2001) 135–142

Organic Electronics

www.elsevier.com/locate/orgel

# Two-dimensional band-like charge transport in α-sexithiophene

J.H. Schön *, Ch. Kloc, S. Berg [1], T. Siegrist, B. Batlogg

*Bell Laboratories, Lucent Technologies, 600 Mountain Avenue, Room MH 1E-318, Murray Hill, NJ 07974-0636, USA*

Received 13 November 2000; received in revised form 11 July 2001; accepted 23 July 2001

**Abstract**

The charge transport in α-sexithiophene single crystals was studied by space charge limited current spectroscopy. Hole mobilities as high as 80 $cm^2/V\,s$ were observed at low temperatures. The strong anisotropic conduction in this material is explained by the molecular packing allowing a strong $\pi$–$\pi^*$ overlap in the molecular planes due to short sulphur–carbon contacts, but almost no molecular overlap at the ends of the molecules. Therefore, the charge carrier can be described as a two-dimensionally extended polaron, which is localized in one molecular plane but delocalized within this plane. The transport mechanism is governed by two-dimensional band-like motion within the planes and a phonon assisted, thermally activated hopping process perpendicular to them. Furthermore, two different single crystalline modifications have been investigated in order to determine the influence of molecular packing on the charge transport. 

*Keywords:* Mobility; Charge transport; Sexithiophene; Polaron; Organic transistor

## 1. Introduction

Organic thin film field-effect transistors based on oligothiophenes and regioregular polythiophene have reached mobilities up to $10^{-1}$ $cm^2/V\,s$ [1–6]. Combined with high on/off current ratios ($>10^6$) these materials are promising candidates for low-cost electronic and optoelectronic devices. Recent reports even demonstrated the monolithical integration of 'plastic' transistors with organic light emitting devices [5,7] and large-scale integration of complementary logic circuits [8]. Despite of this fast technological progress the fundamental understanding of the charge transport mechanism in this new class of materials is still incomplete. Most studies have focused on thin film devices [1,3,9], where disorder and grain boundary effects can mask the intrinsic properties. Only few investigations were carried out on single crystalline materials [10,11]. Recent studies of the charge transport in oligothiophenes indicated hopping transport at high temperatures (above 100 K) [1,3]. However, band-structure and quantum chemical calculations show a strong dispersion of the valence band [12–14] suggesting the possibility of band-like transport in these materials, which was also proposed for low temperatures by the study of thin film devices [1]. Investigations on

* Corresponding author. Tel.: +1-908-582-3052; fax: +1-908-582-4702.

*E-mail address:* hendrik@lucent.com (J.H. Schön).

[1] Present address: Max Planck Institute for Polymer Research, Ackermannweg 10, D-55128 Mainz, Germany.

1566-1199/01/$ - see front matter 
PII: S1566-1199(01)00019-2

polythiophene showed the formation of extended polaron states, nevertheless, the intrinsic temperature dependence of the charge carrier mobility was screened by disorder-induced localization [5].

In this study, we investigated the charge transport in high-quality α-sexithiophene (α-6T) single crystals as a function of temperature and crystal direction by means of space charge limited current (SCLC) spectroscopy. The use of high-quality single crystals minimizes the influence of grain boundaries or disorder and offers the possibility to investigate the intrinsic transport properties of these materials. The influence of molecular packing is explored by the analysis of two different crystallographic phases of α-6T, the high temperature (HT) and low temperature (LT) phase. Furthermore, the investigated oligomer can act as model substance for closely related oligomers with different conjugation length or even polythiophene.

## 2. Experiment

Thin platelets of α-6T single crystals (a few mm thick) were grown from the vapor phase in the flow of hydrogen. Details of the experimental techniques have been reported earlier [15]. Two different modifications, the HT [13] and the LT phase [16], were investigated. The in-plane orientation of the samples was adjusted under crossed polarizers [17]. Ohmic contacts for hole injection were prepared by sputtering of gold through a shadow mask. After the contact preparation the samples were annealed in a flow of hydrogen in order to reduce oxygen-related trapping states. Current–voltage characteristics were measured in the temperature range from 30 to 350 K using a highly sensitive electrometer (Keithley 6517A).

## 3. Results and discussion

### 3.1. In-plane charge transport

Fig. 1 shows a typical current–voltage characteristics of α-6T single crystals at room temperature. Four different regimes can clearly be distinguished

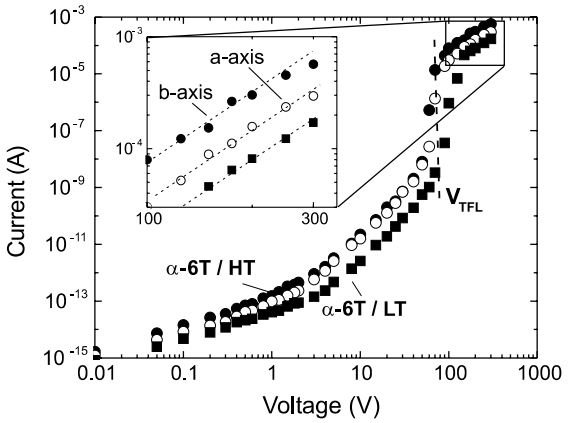


Fig. 1. Current–voltage characteristics at room temperature for an (*a*- and *b*-axis) and an α-6T/LT (*c*-axis) single crystal. The mobility can be determined form the high-voltage region using Child's law, which is magnified in the inset.

[10]: (i) at low voltages the current is proportional to the applied voltage $V$ (ohmic regime), (ii) at higher voltages the current becomes space charge limited and, therefore, proportional to the applied voltage squared. Nevertheless, due to the influence of traps the current is lower than predicted by Child's law, (iii) at $V_{TFL}$ the traps become filled and the current rises by many orders in magnitude and (iv) is then given by the Child's law for trap-free SCLC,

$$j_{SCLC} = \frac{9}{8}\frac{\varepsilon_r \varepsilon_0}{L^3}\mu V^2, \quad (1)$$

where $\varepsilon_0$ is the permittivity of free space, $\varepsilon_r$ the relative dielectric constant, and $L$ the distance between the two contact electrodes. In this regime, when all deep trap levels are filled, the mobility $\mu$ of the charge carriers can be extracted from the current–voltage plot. Typical concentrations in the order of $10^{13}$–$10^{14}$ cm$^{-3}$ have been obtained for deep traps in α-6T.

Fig. 2 shows the measured SCLC mobility along the *b*-axis of different α-6T/HT single crystals as a function of temperature. The differences of the various curves correspond to different densities of shallow trap levels in the α-6T/HT samples. It is worth to mention that these traps could not be filled in the used experimental conditions. At temperatures above 200 K the intrinsic (trap-

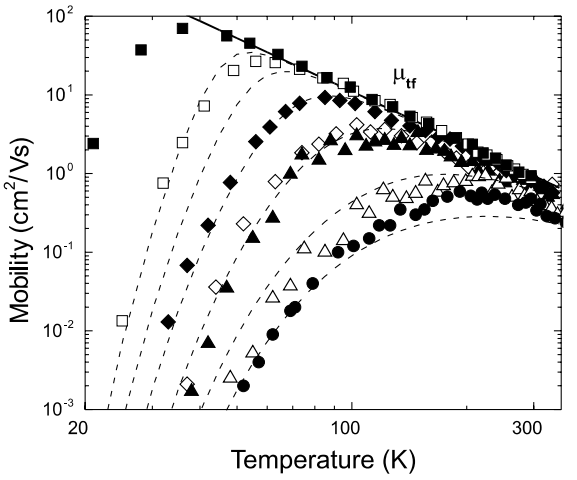


Fig. 2. Mobility as a function of temperature for different α-6T/HT (*b*-axis) single crystals with different concentrations of shallow traps. The trap-free mobility $\mu_{tf}$ (—) is determined from the measured data assuming a trap energy of 50 meV. For comparison the effective mobility is simulated (···) for trap densities in the range from $10^{15}$ to $10^{19}$ $cm^{-3}$.

free) mobility $\mu_{tf}$, which follows a power law ($\mu_{tf} \propto T^{-n}$) is dominant. The measured mobility increases from 0.9 to 80 $cm^2/V\,s$ at 30 K, which is to our knowledge the highest measured value for the mobility in oligothiophenes so far. At lower temperatures the mobility shows a thermally activated behavior due to shallow trapping ($\mu \propto \exp(-E_t/k_bT)T^{-n}$) [18] and the activation energy of the shallow trap can be estimated to 50–60 meV. The temperature dependence of the intrinsic trap-free mobility below 50 K can be estimated from the different samples assuming the same activation energy but different trap concentrations. The dotted lines in Fig. 2 are calculations for various trap densities with an activation energy of 50 meV [18] and an intrinsic mobility (solid line) following a power law of $\mu_{tf} \propto T^{-2.2}$. This power-law dependence of $\mu_{tf}$ indicates a band-like transport mechanism within the molecular planes of α-6T. A similar temperature dependence has been observed in polyacene crystals, like naphthalene, anthracene and pentacene [19–22]. In this case the effective mean free path $\lambda$ at high temperatures (above 200 K) has been approximated by one lattice constant *a* [23,24]. Due to electron–phonon interaction the effective mass $m^*$ of the charge carrier increases significantly with temperature. It can be approximated by an exponential dependence [23,24],

$$m^* = m_0^* \exp\left(\frac{T}{T_0}\right), \tag{2}$$

where the value of $T_0$ is a measure for the energy of the interacting phonons and the electron–phonon coupling parameter [25,26]. The effective mean free path $\lambda$ of the charge carrier can be estimated from the thermal velocity of the charge carrier ($v_{th} = (3k_BT/m^*)^{1/2}$) by [20]

$$\lambda = \frac{\mu}{e}\sqrt{3m^*k_BT}. \tag{3}$$

Therefore, the effective mass in the HT regime, where $\lambda \approx a$, can be calculated from $m^*(T)$ and Eq. (3). Using these values for $m^*(T)$ the LT regime can be fitted according to Eq. (2). A value of $2m_e$ and 72 K were found for $m_0^*$ and $T_0$ for the *b*-axis in α-6T/HT, respectively. Furthermore, an effective bandwidth *W* of 470 meV can be calculated for the charge transport along the *b*-axis in α-6T/HT using

$$W = \frac{4\hbar^2}{m_0^* a^2}. \tag{4}$$

This value is in very good agreement with the bandwidth obtained by extended Hückel theory band structure calculations of 420 meV [12,13] and in reasonable agreement with results of quantum chemical calculations [14]. Employing these obtained values for $m^*$ as a function of temperature, the effective mean free path of the charge carriers $\lambda$ at low temperatures can be estimated from the trap-free mobility $\mu_{tf}$ and Eq. (3). For temperatures below 200 K $\lambda$ increases strongly and reaches values of 70 Å, which is more than 12 lattice constants, at 70 K (see Fig. 3). Hence, the combination of the high-charge carrier mobility, the power-law temperature dependence, the large extracted bandwidth, and the fact that the calculated mean free path exceeds many lattice constants suggest that the charge transport along the molecular planes of α-6T can be successfully described by conventional semiconductor band theory. This implies that the charge carrier can be described by an extended Bloch wave and, therefore, is, at least partly, delocalized. Nevertheless, the increase of

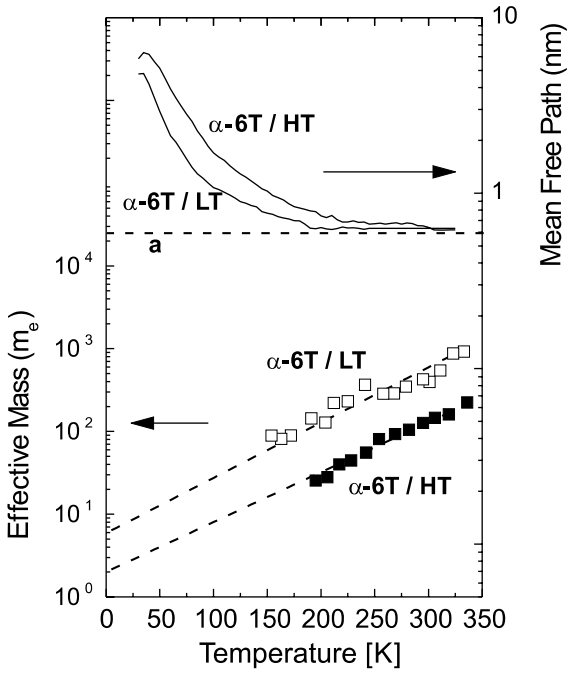


Fig. 3. Effective mass $m^*$ and mean free path $\lambda$ for α-6T/HT (*b*-axis) and α-6T/LT (*c*-axis) as function of temperature. The symbols correspond to the calculated effective mass at high temperatures assuming $\lambda = a$. Using these values the effective mass at low temperatures was obtained using $m^* = m_0^* \exp(T_0/T)$. Employing these values and $\mu_{tf}$ the temperature dependence of $\lambda$ was calculated (—). The dashed lines show the lattice constant $a$ in comparison with $\lambda$.

the effective mass $m^*$ with temperature shows that electron–phonon interaction has to be taken into account, which indicates the polaronic nature of the charge carrier, which might lead to localization at temperatures above room temperature. Although the effective mean free path at high temperatures corresponds to approximately one lattice spacing and the bandwidth narrows significantly, we assume that the conduction does not change with increasing temperature, since the mobility does not exhibit a different temperature dependence up to 350 K.

This observation is in contrast to earlier investigations of oligothiophene thin films, where a thermally activated behavior was observed and therefore incoherent hopping conduction was suggested [3]. Nevertheless, investigations of regioregular poly(hexylthiophene) thin film field-effect transistors indicated the presence of extended states in this high-mobility polymer [5] and optical studies also revealed the two-dimensionality of these materials [27,28]. In addition, these results show that the use of high-quality single crystalline material is an important tool to investigate the intrinsic charge transport properties of organic semiconductors. It minimizes the influence of disorder, impurities and grain boundaries, which is a pre-requisite for the observation of intrinsic material properties.

### 3.2. Anisotropy of the charge transport

In contrast to the conduction along the *b*-axis in α-6T/HT, the charge transport perpendicular to the molecular planes exhibits an activated behavior. Fig. 4 shows the mobility along the *c*-axis, which is perpendicular to the molecular planes, of α-6T/HT as function of temperature. The mobility

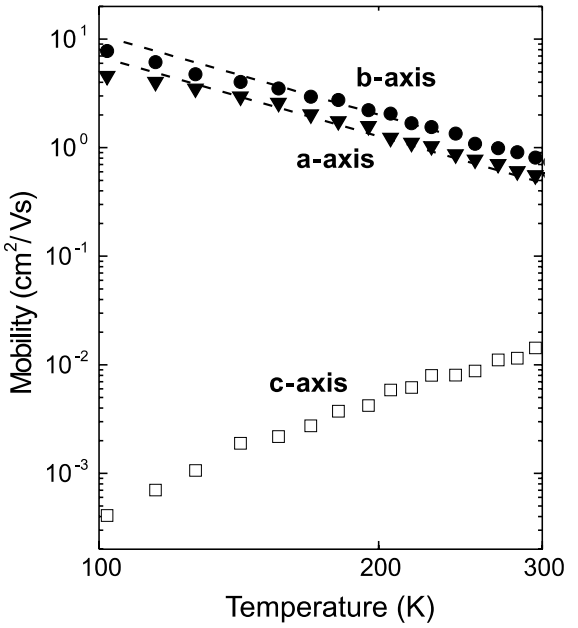


Fig. 4. Mobility in the different crystal directions of α-6T/HT. The dotted lines correspond to the trap-free mobilities in the different directions according to $\mu \propto T^{-n}$ (*a*-, *b*-axis) and $\mu \propto \exp(-E_a/k_B T)$ (*c*-axis) indicating the two-dimensional character of the charge transport.

of a phonon-assisted hopping process can be described by [29]

$$\mu = \mu_0 \exp\left(-\frac{E_a}{2k_B T}\right), \quad (5)$$

where $E_a$ is the activation energy in the case of linear electron–phonon coupling corresponds to half the polaron binding energy $2E_b$ ($E_a = E_b/2$). A value of approximately 40 meV is obtained for $E_a$. Moreover, the anisotropy within the plane (see Figs. 5 and 6) was found to be rather small compared to the anisotropy perpendicular to the molecular planes. The mobility along the *a*-axis is approximately 40% smaller than along the *b*-axis, as shown in Fig. 4. However, it is worth to mention that the direction of the highest mobility does not coincide with one of the crystallographic axis, which can be rationalized from the molecular packing (Fig. 6) [14]. The maximum mobility at room temperature is 1.1 $cm^2/V\,s$. The temperature dependence is very similar for both directions (*a*-axis: $m_0^* = 4.3m_e$, $T_0 = 70$ K). Hence, the charge carrier can be described as two-dimensional polaron, which is localized in one molecular plane but delocalized within the plane. The transport is a two-dimensional coherent band-like motion within the planes and a phonon-assisted, thermally activated hopping process perpendicular to them. This observation is in strong contrast to results presented for pure hydrocarbons, such as pentacene,

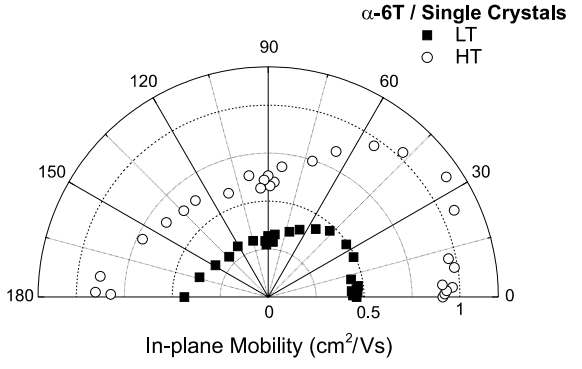


Fig. 5. In-plane mobility at room temperature for both α-6T polymorphic modifications. The 'zero degree direction' corresponds to the *b*-axis (HT) and *c*-axis (LT), respectively. The mobility is measured in the *ab*- and *bc*-plane for the HT and LT modification, respectively.

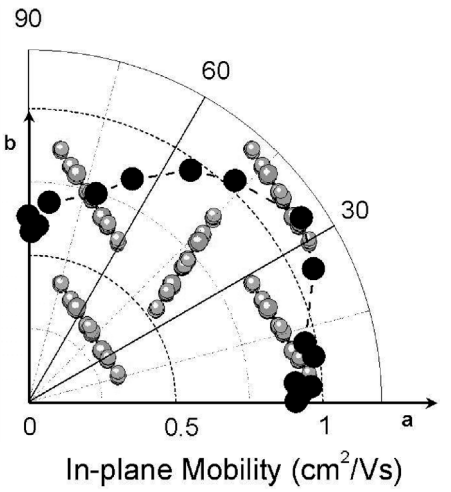


Fig. 6. In-plane mobility at room temperature for the HT polymorph in comparison with the crystallographic structure.

where a three-dimensional band-like transport is observed below room temperature [30]. Nevertheless, the two-dimensional transport has been observed in various oligothiophene materials as well [31]. These differences might be related to the large size of sulfur in the thiophene rings. The importance of the d–π wave function overlap between sulfur and carbon has been pointed out for substituted thiophene polymorphs [32]. This effect might induce a stronger directionality as the pure π–π* interaction observed in hydrocarbons [14]. The parameters of the charge transport are summarized in Table 1.

Table 1
Parameters of the charge transport in α-6T/HT and LT for the three crystallographic directions

| | $\mu_{RT}$ ($cm^2/V\,s$) | $m_0^*$ ($m_e$) | $W$ (meV) | $T_0$ (K) | $E_b$ (meV) |
|---|---|---|---|---|---|
| HT/*a* | 0.6 | 4.3 | 400 | 70 | – |
| HT/*b* | 0.9 | 2 | 470 | 72 | – |
| HT/*c* | 0.015 | – | – | – | 80 |
| LT/*a* | 0.005 | – | – | – | 90 |
| LT/*b* | 0.3 | 9.3 | 145 | 64 | – |
| LT/*c* | 0.45 | 5.9 | 145 | 65 | – |

$\mu_{RT}$: Room temperature mobility; $m_0^*$: LT effective mass; $W$: bandwidth; $T_0$: temperature dependence of $m^*$; and $E_b$: polaronic binding energy.

### 3.3. Influence of molecular packing

The crystal structures of α-6T/HT and LT are shown in Fig. 7. The larger tilting angle in the HT phase results in a staggering of the α-6T molecules. Therefore, the intermolecular distances found in both polymorphs are quite different. Especially, the closest lateral intermolecular contacts (carbon–sulphur distances) are shorter for the HT modification due to this different stacking of the molecules. In α-6T/LT the lateral contacts are formed from each thiophene subunit to its corresponding subunit on the adjacent molecules, while in α-6T/HT, the shift of the molecule by one thiophene subunit allows the contacts to form between the first and the next thiophene subunit [33,34]. Extended Hückel band-structure calculations for both α-4T polymorphs, which show the same packing differences, showed that the dispersion of the valence band in the LT phase is significantly smaller (0.17 eV) than in the HT phase (0.45 eV) [33]. Since the latter dispersion is very similar to that found in α-6T/HT (0.42 eV) [12,13], we assume that 0.17 eV is a good approximation for the dispersion in α-6T/LT. This smaller dispersion results in a larger effective mass (Eq. (4)) and therefore in a smaller mobility, as observed experimentally (see Fig. 8). The LT bandwidth for the LT phase has been estimated using the same assumptions as for the HT polymorph (see Section 3.1). An effective mass $m_0^*$ of $5.9m_e$, corresponding to a bandwidth of 145 meV, and a value of 65 K for $T_0$ have been obtained, which is in very good agreement with the band-structure calculations. Furthermore the smaller value of $T_0$ suggests a stronger electron–phonon coupling in the LT phase. The in-plane anisotropy in the LT phase is similar to that found in the HT phase: $m_c$:$m_b$ is 1.5:1 (see Figs. 5 and 6). Due to the different packing of both modifications, the *c*-axis in the LT phase corresponds to the *b*-axis in the HT phase

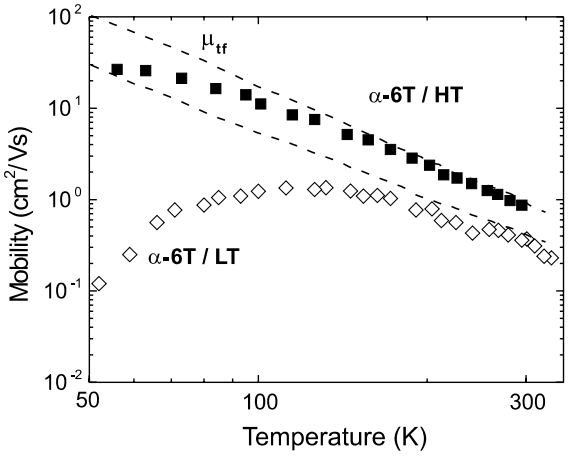


Fig. 8. Temperature dependence of the mobility for the high mobility directions in α-6T/HT and α-6T/LT showing the influence of different molecular packing.

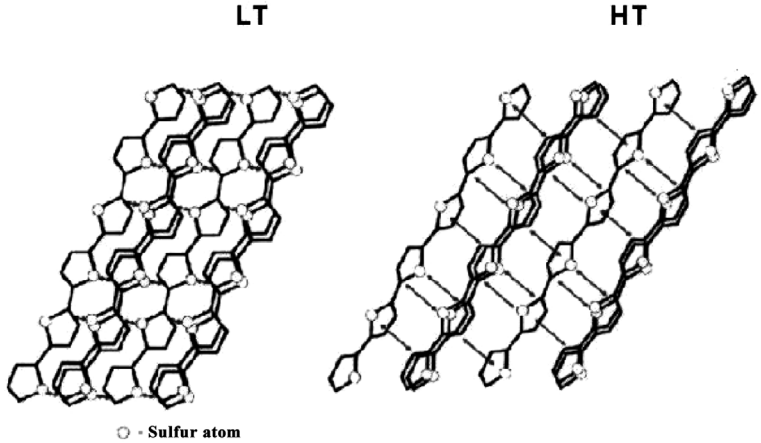


Fig. 7. Crystal structures of α-6T/HT [10] and α-6T/LT [13]. The main difference between both polymorphs is the tilting angle of the molecule. The different shortest sulphur–carbon contacts are indicated by dashed lines.

(short axis in-plane) and the *b*-axis of LT to the *a*-axis of HT (long axis in-plane). The anisotropy between the conduction in-plane and perpendicular to the plane is slightly higher for the LT phase. The mobility also shows the typical thermal activation for phonon-assisted hopping (Eq. (5)). The obtained value of 85 meV for the polaron binding energy is similar to that for the HT polymorph. The parameters of the charge transport for both modifications are summarized in Table 1.

## 4. Summary and conclusion

The charge transport in α-6T single crystals was investigated by means of SCLC spectroscopy. The charge transport shows a strong two-dimensional character. The charge carrier can be described as two-dimensional polaron, which is localized in one molecular plane but delocalized within the plane. The conduction mechanism is a two-dimensional coherent band-like motion within the planes ($\mu \propto T^{-2.2}$) and a phonon assisted, thermally activated hopping process perpendicular to them. These experimental findings are in line with band-structure calculations, which show that the valence band displays a significant dispersion along the short axes, but almost no dispersion perpendicular to that. In addition, two different single crystalline phases were studied in order to evaluate the influence of the molecular packing on the mobility. It was found, that short sulphur–carbon distances between the different α-6T are essential for a strong dispersion of the conduction band and therefore for a high mobility. Hence, optimizing the molecular assembly of oligothiophenes in thin films due to process parameters or different substrate modifications might lead to further improvement of electronic devices.

## Acknowledgements

We like to thank Z. Bao, E. Bucher, E.A. Chandross, A. Dodabalapur, R.C. Haddon and H.E. Katz for various helpful discussions. One of the authors (J.H.S.) gratefully acknowledges financial support by the 'Deutsche Forschungsgemeinschaft'.

## References

[1] L. Torsi, A. Dodabalapur, L.J. Rothberg, A.W.P. Fung, H.E. Katz, Science 272 (1996) 1462.
[2] F. Garnier, G. Horowitz, D. Fichou, A. Yassar, Synth. Met. 81 (1996) 163.
[3] K. Waragai, H. Akimichi, S. Hotta, H. Kano, Phys. Rev. B 52 (1995) 1786.
[4] J. Paloheimo, P. Kuivalainen, H. Stubb, E. Vuorimaa, P. Yli-Lahti, Appl. Phys. Lett. 56 (1990) 1157.
[5] H. Sirringhaus, N. Tessler, R.H. Friend, Science 280 (1998) 1741.
[6] G. Horowitz, M.E. Hajlaoui, Adv. Mater. 12 (2000) 1046.
[7] A. Dodabalapur, Z. Bao, A. Makhija, J.G. Laquindanum, V.R. Raju, Y. Feng, H.E. Katz, J. Rogers, Appl. Phys. Lett. 73 (1998) 142.
[8] B. Crone, A. Dodabalapur, Y.-Y. Lin, R.W. Filas, Z. Bao, A. LaDuca, R. Sarpeshkar, H.E. Katz, W. Lin, Nature 403 (2000) 521.
[9] A.R. Brown, C.P. Jarrett, D.M. de Leeuw, M. Matters, Synth. Met. 88 (1997) 37.
[10] J.H. Schön, Ch. Kloc, R.A. Laudise, B. Batlogg, Phys. Rev. B 58 (1998) 12952.
[11] W.A. Schoonveld, J. Vrijmoeth, T.M. Klapwijk, Appl. Phys. Lett. 73 (1998) 3884.
[12] T. Siegrist, R.M. Fleming, R.C. Haddon, R.A. Laudise, A.J. Lovinger, H.E. Katz, P. Bridenbaugh, D.D. Davis, J. Mater. Res. 10 (1995) 2170.
[13] R.C. Haddon, T. Siegrist, R.M. Fleming, P.M. Bridenbaugh, R.A. Laudise, J. Mater. Chem. 5 (1995) 1719.
[14] J. Cornil, J.-P. Calbert, D. Beljonne, R. Silbey, J.-L. Bredas, Adv. Mater. 12 (2000) 978.
[15] Ch. Kloc, P.G. Simpkins, T. Siegrist, R.A. Laudise, J. Cryst. Growth 182 (1997) 416.
[16] G. Horowitz, B. Bachet, A. Yassar, P. Lang, F. Demanze, J.-L. Fave, F. Garnier, Chem. Mater. 7 (1995) 1337.
[17] J. Vrijmoeth, R. Stok, R. Veldman, W.A. Schoonveld, T.M. Klapwijk, J. Appl. Phys. 83 (1998) 3816.
[18] N. Karl, in: K. Sumino (Ed.), Defect Control in Semiconductors, vol. 2, Elsevier, Amsterdam, 1990, p. 1725.
[19] N. Karl, in: O. Madelung, M. Schulz, H. Weiss (Eds.), Organic Semiconductors, Landolt-Börnstein, New Series Vol. 17, Semiconductors Subvolume 17i, Springer, Berlin, 1985, pp. 106–218.
[20] W. Warta, N. Karl, Phys. Rev. B 32 (1985) 1172.
[21] J.H. Schön, S. Berg, Ch. Kloc, B. Batlogg, Science 287 (2000) 1022.
[22] J.H. Schön, Ch. Kloc, B. Batlogg, Science 288 (2000) 2338.
[23] E.A. Silinsh, G.A. Shlihta, A.J. Jurgis, Chem. Phys. 155 (1991) 389.
[24] E.A. Silinsh, G.A. Shlihta, A.J. Jurgis, Chem. Phys. 138 (1989) 347.

[25] C.E. Sweneberg, M. Pope, Chem. Phys. Lett. 287 (1998) 535.
[26] M.W. Wu, E.M. Conwell, Chem. Phys. Lett. 266 (1997) 363.
[27] R. Österbacka, C.P. An, X.M. Jiang, Z.V. Vardeny, Science 287 (2000) 839.
[28] H. Sirringhaus, P.J. Brown, R.H. Friend, M.M. Nielsen, K. Bechgaard, B.M.W. Langeveld-Voss, A.J.H. Spiering, R.A.J. Janssen, E.W. Meijer, P. Herwig, D.M. De Leeuw, Nature 401 (1999) 685.
[29] M. Pope, C.E. Swenberg, Electronic Processes in Organic Crystals, second ed., Clarendon Press, Oxford, 1999.
[30] J.H. Schön, Ch. Kloc, B. Batlogg, Phys. Rev. B 63 (2001) 245201.
[31] J.H. Schön, Ch. Kloc, D. Fichou, B. Batlogg, Phys. Rev. B 64 (2001) 035209.
[32] J. Widany, G. Daminelli, A. Di Carlo, P. Lugli, G. Jungnickel, M. Elstner, Th. Frauenheim, Phys. Rev. B 63 (2001) 233204.
[33] T. Siegrist, Ch. Kloc, R.A. Laudise, H.E. Katz, R.C. Haddon, Adv. Mater. 10 (1998) 379.
[34] L. Antolini, G. Horowitz, F. Kouki, F. Garnier, Adv. Mater. 10 (1998) 382.